

MoKD: Multi-Task Optimization for Knowledge Distillation

Zeeshan Hayder^{1,2}, Ali Cheraghian^{1,2}, Lars Petersson¹, Mehrtash Harandi³

¹Data61, CSIRO, Australia, ²Australian National University, ³Monash University

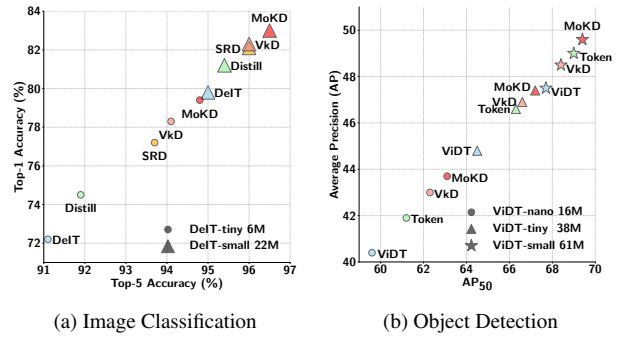
{zeeshan.hayder, ali.cheraghian, lars.petersson}@data61.csiro.au, mehrtash.harandi@monash.edu

Abstract

Compact models can be effectively trained through Knowledge Distillation (KD), a technique that transfers knowledge from larger, high-performing teacher models. Two key challenges in Knowledge Distillation (KD) are: 1) balancing learning from the teacher’s guidance and the task objective, and 2) handling the disparity in knowledge representation between teacher and student models. To address these, we propose Multi-Task Optimization for Knowledge Distillation (**MoKD**). MoKD tackles two main gradient issues: a) **Gradient Conflicts**, where task-specific and distillation gradients are misaligned, and b) **Gradient Dominance**, where one objective’s gradient dominates, causing imbalance. MoKD reformulates KD as a multi-objective optimization problem, enabling better balance between objectives. Additionally, it introduces a subspace learning framework to project feature representations into a high-dimensional space, improving knowledge transfer. Our MoKD is demonstrated to outperform existing methods through extensive experiments on image classification using the ImageNet-1K dataset and object detection using the COCO dataset, achieving state-of-the-art performance with greater efficiency. To the best of our knowledge, MoKD models also achieve state-of-the-art performance compared to models trained from scratch.

1. Introduction

Large deep learning models have achieved remarkable success in computer vision tasks, but their adoption is often limited by high computational costs, making it challenging to deploy on resource-constrained systems like edge devices and mobile phones. To address this, there has been a growing interest in reducing model size while maintaining performance. One effective approach achieving this is so called *knowledge distillation* (KD) [8, 25, 42, 48], where a smaller model, called the student, is trained to mimic the outputs of a larger, pre-trained model, known as the teacher. This technique allows the student model to learn from the teacher’s knowledge, enabling it to achieve competitive performance



(a) Image Classification

(b) Object Detection

Figure 1. **a)** Top-1 and top-5 validation classification accuracy of student models trained for 300 epochs on ImageNet-1K with a pre-trained RegNetY-160 teacher. Model size is indicated by shape, with smaller circles for ViDT-tiny and larger ones for ViDT-small. **b)** Object detection results (AP and AP@50) for student models trained for 50 epochs on COCO with a pre-trained ViDT-base teacher. Model size is indicated by shape, with smaller circles for ViDT-nano and larger stars for ViDT-small. As can be seen, MoKD achieves the best performance in every scenario.

with fewer parameters, making it more suitable for deployment on devices with limited resources. In a typical KD pipeline, this process involves a task-specific loss function, such as classification or object detection, alongside a mechanism to transfer knowledge from the teacher to the student.

Earlier works in KD [11, 45] focused on using the teacher’s predictions as the ground-truth labels for the student model. However, this approach has limitations, as the teacher’s output is often overly compressed, and distilling knowledge solely from the final logits restricts the amount of useful information that can be transferred. To address this, later KD techniques [2, 10, 28] shifted toward distilling knowledge from the teacher’s feature space, enabling a more flexible and informative transfer process. This is typically achieved by heuristic design choices and additional hyperparameters that need task-specific tuning. Despite advancements, feature-based KD approaches [3, 4, 29] still struggle with effectively transferring knowledge from complex teacher models to simpler student models due to the inconsistency between the optimization objectives of ground-truth supervision and the distillation targets.

The optimization inconsistency is a key factor limiting the efficiency of teacher mimicking [4, 15, 37, 37] approaches. The primary issue limiting the performance of these approaches is two-fold. First, **Gradient Conflicts (GrC)** arise when the gradients of the task-specific objective and the distillation process are misaligned. Second, **Gradient Dominance (GrD)** occurs when the gradient magnitude of one objective (e.g., either distillation or task-specific) dominates the learning process, causing an imbalance. To address all of these issues, we propose a novel knowledge distillation optimization strategy. Specifically, we frame the problem as a multi-task optimization, which not only efficiently resolves gradient conflicts during training but also ensures a Pareto optimal [15] solution. This results in a training strategy that eliminates the need for manually tuning hyperparameters to balance the contributions of each loss function. Instead, it dynamically learns the contribution of each loss function, adapting between task-specific and distillation-specific objectives throughout the training.

Another key factor that is crucial for effective distillation is learning the topology and local structure of the teacher’s latent space. It enhances knowledge transfer not only from the highest scoring prediction but also from the remaining outputs, known as dark knowledge distillation. Preserving the student model’s structure is important, [29] demonstrates that using an adaptation module can enhance the flow of information between the teacher and student. These modules are used during training to facilitate learning but are removed afterwards, ensuring that the student model’s size and structure remain unchanged. [29] also suggests that using orthogonal adapters and normalization techniques are essential for this approach. However, it has certain limitations. Imagine the teacher has a feature space defined by features (f_1, f_2) . Now, consider a student whose features are (f_2, f_1) . This student is able to perfectly capture the teacher’s space, but only if it’s rotated. In standard feature distillation, the goal is to teach the student to learn the feature set (f_1, f_2) from the teacher’s features (f_2, f_1) . However, this can be very challenging because the features are not aligned — it’s like trying to learn a rotated version of the feature space, which may not be easy to achieve. We improve [29] by equipping the flow of knowledge via projections into a high-dimensional space.

In this paper, we propose a novel multi-task learning strategy for knowledge distillation in an end-to-end manner, which improves the flow of knowledge. It is more efficient, requiring fewer epochs to achieve a performance comparable to state-of-the-art methods [21, 29, 31, 33]. Additionally, we propose learning both the student and teacher subspaces through a plug-and-play adaptation module that enhances the knowledge distillation process. To this end, we evaluated our method on the challenging ImageNet classification task, where MoKD achieves state-of-the-art results,

as shown in Fig. 1a. Additionally, we tested our approach on the object detection task, where MoKD consistently outperforms existing baselines across various teacher models, as depicted in Fig. 1b. In summary, the contributions of this paper are as follows:

- We introduce a novel optimization strategy that automatically adjusts the contribution of task-specific and distillation-specific loss functions, eliminating the need for manual hyper-parameter tuning.
- We propose a novel plug-and-play module for learning student and teacher subspaces and aligning them in a high-dimensional space. This enables a more flexible alignment and improves knowledge transfer efficiency for enhanced positive and dark knowledge distillation.
- We have conducted extensive experiments on object classification and detection, achieving state-of-the-art results on both tasks, as depicted in Fig. 1. The ablation experiments also show that MoKD is robust to different teacher-student distillation scenarios.

2. Related work

This section explores knowledge distillation (KD) [11] techniques, focusing on the use of logits, CNN features, and transformer features (or tokens). Additionally, it examines subspace learning methods for KD and multi-task approaches relevant to the MoKD.

Logit-based knowledge distillation: Logit-based techniques have traditionally emphasized the distillation process by utilizing solely the output logits. For instance, [45] uses an ensemble of students who learn collaboratively, while [22] employs a multi-stage distillation with a teacher assistant network. Additionally, [46] introduces a decoupling strategy, applying distillation to different branches of the teacher’s output individually. However, the logit-based distillation has key limitations: it transfers only the final layer’s outputs, missing rich feature representations from earlier layers, and limits the student’s ability to generalize and learn deeper knowledge. The student model also struggles to align the teacher’s context-specific predictions with the task-specific objectives, leading to suboptimal learning.

Feature-based knowledge distillation: Feature-based KD focuses on utilizing intermediate layer features to relay knowledge from the teacher to the student model [39, 40]. Firstly, introduced in [28], as a stage-wise training approach, where the student network is first trained up to a specific layer and then gradually distills the knowledge from the teacher. Building on this, [10] introduces a filtering strategy using margin ReLU to eliminate redundant information flow between the teacher’s and student’s features. In this method, the distillation loss aligns the transformed features of both models, their respective feature positions, and the distance function, improving the efficiency of knowledge transfer. [3] investigates the connection

paths between different levels of the teacher and student networks, highlighting their crucial role in enhancing the distillation process. Additionally, a diffusion model-based method in [13] reduces the noise in student models before distilling the knowledge from a teacher. Furthermore, [38] introduces a new norm and direction loss function alongside the typical KD loss. However, feature-based distillation approaches are limited in transferring knowledge as they struggle to capture long-range dependencies and global context, which are crucial for understanding the teacher’s latent space.

Token-based knowledge distillation: [36] introduced the first convolution-free transformer model for object classification, using token distillation for the student model to learn from the teacher via attention. [32, 33] proposed token-matching distillation for object detection, where the student mimics the teacher’s tokens by training with the same number of patch and detection tokens. However, simple token-mimicking is suboptimal. To improve this, [27] introduced a multi-teacher distillation method, where lightweight teachers with different biases co-advise the student transformer, reducing conflicting objectives. [9] proposed a manifold-based approach, projecting both student and teacher tokens into a shared space for fine-grained distillation. Despite this, transferring dark knowledge remains a challenge. Addressing this, [41] introduced a normalizing strategy for non-target logits in the KD loss and explored self-distillation. However, these single-stage approaches have difficulties balancing the competing objectives of task learning and distillation. [4] introduced a two-stage approach to address this, where distillation is applied to the early intermediate layers in the first stage, and the transformer completes the remaining epochs without distillation to fully exploit its learning capacity in the second stage. However, this approach is ad hoc, and in this paper, we propose an end-to-end strategy that leverages multi-task optimization to address this challenge.

Subspace learning for knowledge distillation: Directly mimicking the teacher’s features or tokens can be challenging. As a result, there is a need to introduce an intermediate step to facilitate the Knowledge Distillation (KD) process during training. To this end, [21] explores the idea of learning a plug-and-play module to implicitly encode the relational gradient. They proposed a normalization and projector-based method for cross-batch knowledge transfer. [29] extended this approach with orthogonal projections, relying on Hilbert spaces [43] for distillation. However, these approaches impose the restrictive constraint of positive-definite metrics. This limitation hinders seamless knowledge transfer for distillation. In this paper, we propose using indefinite spaces, offering greater flexibility and enabling smoother knowledge transfer.

Multi-task optimization: Multi-task optimization tech-

niques were introduced to address the challenge of conflicting objectives when learning multiple tasks. The simplest form of multi-task optimization (MTO) involves re-weighting loss functions based on manually designed criteria [6, 14]. However, these methods are often heuristic and lack strong theoretical foundations. In contrast, gradient manipulation methods [17–19, 30, 44] for MTO aim to generate a new update vector at each optimization step by linearly combining the gradients from different tasks. [30] suggests using an upper bound for the multi-task loss to enhance optimization efficiency, while [44] projects a task’s gradient onto the normal plane of conflicting tasks’ gradients. [17, 19] introduce a closed-form solution that minimizes the average loss while regularizing the algorithm’s trajectory. Lastly, [18] proposes a fast dynamic weighting method that balances task losses with constant time and space complexity. While these methods have been applied to multi-task learning, MoKD focuses specifically on knowledge distillation. We treat the knowledge distillation process as a multi-task optimization problem, distinct from the previous traditional multi-task setting. To the best of our knowledge, none of the existing KD approaches benefit from these gradient-based multi-task optimization methods.

3. Method

We introduce a Multi-task Optimization approach for Knowledge Distillation (MoKD), with a specific focus on resolving the conflicting objectives in the KD process. Figure 2 shows an illustration of our proposed framework.

Problem formulation. We aim to transfer knowledge from a high-capacity teacher model with parameters ϕ , to a more compact model student, with parameters θ , focusing chiefly on classification and detection tasks in visual recognition. We show the training data with $\mathcal{S} = \{(\mathbf{x}_i, \mathbf{y}_i)\}_{i=1}^N$, with $\mathbf{x}_i \in \mathbb{R}^d$ being the i -th input instance and \mathbf{y}_i the corresponding target (e.g. a class label, bounding box). Our goal is to train the student model to effectively mimic the behavior of the teacher model over the dataset \mathcal{S} .

Effectively performing knowledge distillation requires balancing two objectives: the student must learn from two supervisory signals (e.g., one from the teacher and one from the task). We represent the teacher’s loss as L_{distill} and the task’s loss as L_{task} . While we will define these more specifically for image classification and object detection in the appendix, we provide their general forms here:

$$L_{\text{distill}}(\theta) \triangleq \mathbb{E}_{(\mathbf{x}, \mathbf{y}) \sim \mathcal{S}} \ell_{\text{distill}}(f_s(\mathbf{x}; \theta), f_t(\mathbf{x}; \phi)) \quad (1)$$

$$L_{\text{task}}(\theta) \triangleq \mathbb{E}_{(\mathbf{x}, \mathbf{y}) \sim \mathcal{S}} \ell_{\text{task}}(f_s(\mathbf{x}; \theta), f_t(\mathbf{x}; \phi)) \quad (2)$$

The conventional KD approaches (e.g., [12, 47]) train the student model by optimizing the loss as

$$L_{\text{tot}}(\theta) \triangleq \alpha_1 L_{\text{distill}}(\theta) + \alpha_2 L_{\text{task}}(\theta), \quad (3)$$

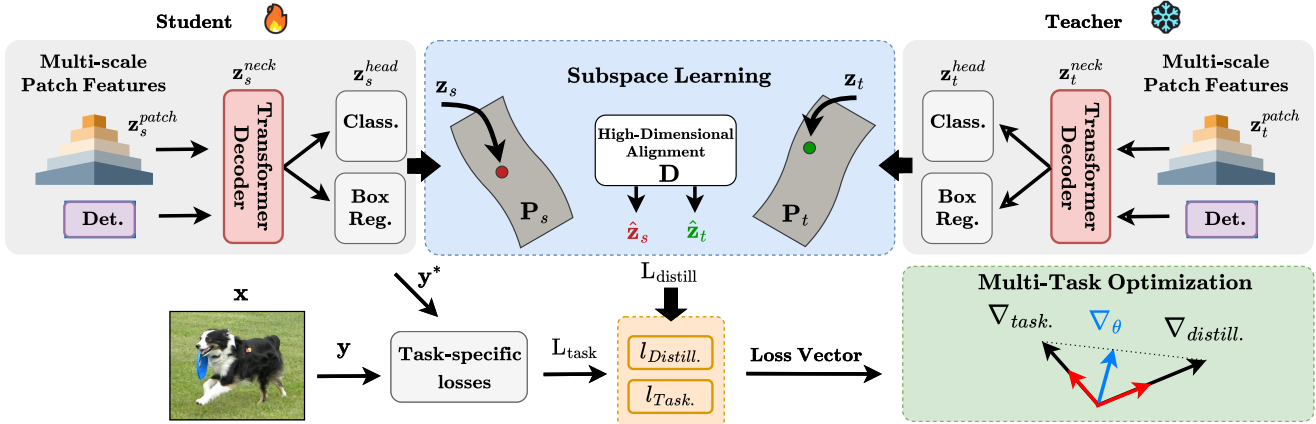


Figure 2. In MoKD, the teacher and student models simultaneously process the input image \mathbf{x} . The teacher’s features (\mathbf{z}_t), and the student’s (\mathbf{z}_s), are aligned using subspace learning. This is achieved via learning two separate subspaces — \mathbf{P}_t for the teacher and \mathbf{P}_s for the student — tailored to each model. We also use an indefinite metric \mathbf{D} for alignment. We formulate training as a multi-objective optimization (MOO) and develop an algorithm to ensure reducing the distillation loss $\mathcal{L}_{\text{distill}}$ and the task-specific loss $\mathcal{L}_{\text{task}}$ towards Pareto optimality.

where $\alpha_1, \alpha_2 \in \mathbb{R}_+$ are the combination weights and hyperparameters of the model. The gradient of $L_{\text{tot}}(\theta)$ is

$$\mathbf{g}_{\text{tot}} = \nabla \mathcal{L}_{\text{tot}}(\boldsymbol{\theta}) = \alpha_1 \mathbf{g}_{\text{dist}} + \alpha_2 \mathbf{g}_{\text{task}} \quad (4)$$

where $\mathbf{g}_{\text{dist}} = \nabla \mathcal{L}_{\text{distill}}(\theta)$ is the gradient of the distillation loss, and $\mathbf{g}_{\text{task}} = \nabla \mathcal{L}_{\text{task}}(\theta)$ is the gradient of the task loss.

Minimizing a single loss function, as in Equation (3), for joint training introduces the following challenges:

Gradient Conflict (GrC). This occurs when the gradients of the distillation loss and the task loss conflict with each other. Mathematically, GrC happens when $\langle \mathbf{g}_{\text{dist}}, \mathbf{g}_{\text{task}} \rangle < 0$. During the optimization of the total loss $L_{\text{tot}}(\theta)$, the occurrence of GrC leads to conflicting gradient updates. Specifically, the total gradient \mathbf{g}_{tot} may contradict either \mathbf{g}_{dist} or \mathbf{g}_{task} , causing detrimental effects on one or both objectives. This conflict can exacerbate the learning dynamics, particularly in complex vision tasks such as object detection, by introducing unnecessary complexity into the training process. In Appendix C.4(a), we examine the phenomenon of GrC in the context of knowledge distillation for object detection [29]. The figure illustrates how the gradients from \mathbf{g}_{dist} and \mathbf{g}_{task} are in direct conflict, as evidenced by their negative values.

Gradient Dominance (GrD). It arises when the gradients have significantly different magnitudes, leading one to dominate the update. When minimizing $L_{\text{tot}}(\theta)$, this imbalance may cause one objective to be completely neglected, as the update direction is primarily determined by the larger gradient. In Appendix C.4(b), we study GrD for the knowledge distillation baseline for object detection [29]. The figure shows $\frac{\|g_{\text{dist}}\|}{\|g_{\text{task}}\|}$ plotted on y-axis in a log-scale. It is evident that the gradients of g_{task} are dominating the overall learning process. Lastly, tuning the hyperparameters α_1 and α_2

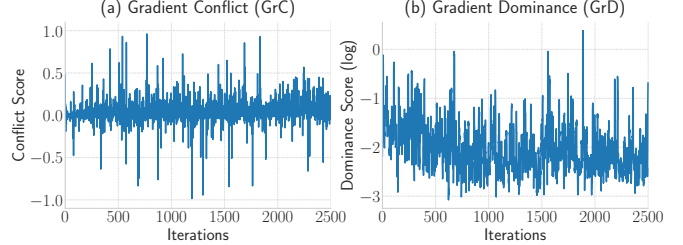


Figure 3. **Gradient Dynamics** analysis. a) Conflict score is calculated as $\langle g_{\text{dist}}, g_{\text{task}} \rangle$. A negative score shows strong disagreement. b) The dominance score is calculated as $\frac{\|g_{\text{dist}}\|}{\|g_{\text{task}}\|}$ and plotted in log-scale. The lower score represents strong dominance.

might become extremely tricky as the norm of gradients varies throughout optimization.

To address the aforementioned challenges, we advocate for the use of multi-objective optimization in KD. Specifically, we formulate the training process as optimizing the objective vector $L_{\text{tot}}(\theta) = (L_{\text{distill}}(\theta), L_{\text{task}}(\theta))^{\top}$. The goal is to find a solution θ^* on the Pareto front, *i.e.*, a solution that is not dominated by any other parameter vector $\tilde{\theta}$. Formally, θ^* is Pareto optimal if is no $\tilde{\theta}$ such that

$$\begin{pmatrix} \mathcal{L}_{\text{distill}}(\tilde{\theta}) \\ \mathcal{L}_{\text{task}}(\tilde{\theta}) \end{pmatrix} \preceq \begin{pmatrix} \mathcal{L}_{\text{distill}}(\theta^*) \\ \mathcal{L}_{\text{task}}(\theta^*) \end{pmatrix} \quad (5)$$

The notation $a \preceq b$ here means that vector a achieves a lower value for all its elements simultaneously over b . As we will discuss in the next section, formulating KD using the proposed algorithm addresses both GrC and GrD by aligning the gradients. Furthermore, the use of MOO mitigates the difficulty of hyperparameter tuning, as it eliminates the need to manually define α_1 and α_2 .

3.1. KD as a multi-objective optimization

Inspired by [18] and at time t , we update the student model via $\theta_{t+1} = \theta_t - \eta g_t$, where $\eta \in \mathbb{R}_+$ is the learning step size. We define the rate of improvement for the distillation and task losses as:

$$\begin{aligned} r_{\text{dist}}(g_t) &= \frac{L_{\text{distill}}(\theta_t) - L_{\text{distill}}(\theta_{t+1})}{L_{\text{distill}}(\theta_t)}, \\ r_{\text{task}}(g_t) &= \frac{L_{\text{task}}(\theta_t) - L_{\text{task}}(\theta_{t+1})}{L_{\text{task}}(\theta_t)}. \end{aligned} \quad (6)$$

In essence, $r_{\text{dist}}(g_t)$ and $r_{\text{task}}(g_t)$ measure how much each loss can be improved by moving the parameters with $-\eta g_t$. A larger value of r_{dist} or r_{task} implies the associated task has been improved more. Our goal is to determine an update g_t that maximizes the improvement over the worst-case rate. This can be achieved using a min-max optimization as:

$$\max_{g_t \in \mathbb{R}^n} \min_{i \in \{\text{dist, task}\}} \frac{1}{\gamma} r_i(g_t) - \frac{1}{2} \|g_t\|^2. \quad (7)$$

Here, $\gamma \in \mathbb{R}_+$ is a weighting hyperparameter. As shown in [18], the solution of Equation (7) can be obtained via solving its dual problem as (see proposition 3.1 in [18]). Define $\pi = (\pi_1, \pi_2)^\top$ on the simplex Δ (i.e., $\pi_1 + \pi_2 = 1, \pi_1, \pi_2 \geq 0$), and let $J_t \in \mathbb{R}^{n \times 2}$ be

$$J_t = [\nabla \log(L_{\text{distill}}(\theta_t)) \mid \nabla \log(L_{\text{task}}(\theta_t))]^\top \quad (8)$$

Then

$$\pi_t^* \in \arg \min_{\pi \in \Delta} \frac{1}{2} \|J_t \pi\|^2, \quad (9)$$

and $g_t = J_t \pi^* = \pi_1 \nabla \log(L_{\text{distill}}(\theta_t)) + \pi_2 \nabla \log(L_{\text{task}}(\theta_t))$.

Theoretical Properties. The problem formulation in 9 admits an analytical solution, unlike the general case studied in [18]. In this part, we establish key theoretical properties of the obtained update direction g^* .

Theorem 3.1 (Closed Form Solution). *Let $J_t = [\nabla \log(L_{\text{distill}}(\theta_t)), \nabla \log(L_{\text{task}}(\theta_t))] \in \mathbb{R}^{n \times 2}$. The closed-form solution to the optimization problem*

$$\begin{aligned} \pi^* &\in \arg \min_{\pi} \frac{1}{2} \|J_t \pi\|^2 \\ \text{s.t. } \pi_1 + \pi_2 &= 1 \end{aligned} \quad (10)$$

is given by

$$\pi_1^* = \frac{g_{22} - g_{12}}{g_{11} + g_{22} - 2g_{12}}, \quad (11)$$

$$\pi_2^* = \frac{g_{11} - g_{12}}{g_{11} + g_{22} - 2g_{12}}, \quad (12)$$

where $G = J_t^\top J_t$ is the Gram matrix:

$$G = \begin{bmatrix} g_{11} & g_{12} \\ g_{21} & g_{22} \end{bmatrix},$$

with elements

$$\begin{aligned} g_{11} &= \|\nabla \log(L_{\text{distill}}(\theta_t))\|^2, \\ g_{12} &= g_{21} = \langle \nabla \log(L_{\text{distill}}(\theta_t)), \nabla \log(L_{\text{task}}(\theta_t)) \rangle, \\ g_{22} &= \|\nabla \log(L_{\text{task}}(\theta_t))\|^2. \end{aligned}$$

The closed-form nature of this solution allows for efficient computation of the optimal weighting factors. One key property of the derived solution is that the update direction aligns with both objectives, ensuring that both the distillation and task losses are reduced simultaneously. This directly addresses GrC by preventing destructive interference between the two gradients.

Corollary 3.2 (Alignment of g^*). *Define $g_1 = \nabla \log(L_{\text{distill}}(\theta_t))$ and $g_2 = \nabla \log(L_{\text{task}}(\theta_t))$. Then the update direction $g^* = \pi_1 g_1 + \pi_2 g_2$ for π^* defined in Equation (4) is aligned with both g_1 and g_2 .*

Another key property of the proposed solution is that it enforces equal contribution of the update direction to both gradients, effectively addressing GrD.

Corollary 3.3 (Equal Contribution of g^* to Both Losses). *In Corollary B.2, we showed that*

$$\langle g^*, g_1 \rangle = \langle g^*, g_2 \rangle = \frac{g_{11}g_{22} - g_{12}^2}{\|g_1 - g_2\|^2}.$$

This implies that the update direction contributes equally to the descent of both the distillation and task losses, effectively mitigating gradient dominance.

An important aspect of any gradient-based optimization method is ensuring that update magnitudes remain within a controlled range to prevent vanishing or exploding gradients. Our solution satisfies both a lower and an upper bound on $\|g^*\|$, ensuring stability during training.

Corollary 3.4 (Lower Bound on $\|g^*\|$). *The norm of the optimal update direction g^* satisfies the lower bound:*

$$\|g^*\| \geq \frac{1}{\sqrt{2}} \min(\|g_1\|, \|g_2\|). \quad (13)$$

This implies that the update magnitude remains controlled and does not collapse under gradient imbalance.

Corollary 3.5 (Upper Bound on $\|g^*\|$). *The norm of the optimal update direction g^* satisfies the upper bound:*

$$\|g^*\| \leq \frac{\|g_1\| \|g_2\|}{\|g_1\| - \|g_2\|}. \quad (14)$$

As such, the magnitude of the updates does not grow excessively when the gradients have different scales.

Finally, we observe that the algorithm’s convergence is ensured by the general theoretical framework outlined in [18]. As our formulation aligns with it, the proposed optimization is guaranteed to converge to a Pareto front.

Practical Implementation. Despite having strong theoretical properties, MTL algorithms, including the one we have developed above, require access to per task gradient, in our case access to $\mathbf{J} = [\nabla \log(L_{\text{distill}}(\theta_t)), \nabla \log(L_{\text{task}}(\theta_t))]$. This incurs performing two backpropagation per iteration, which is not desired. Instead, and as shown in [18], one can advocate to amortizing the training. This leads to an approximation to the algorithm while ensuring that an extra backprop step is not required. In short, the parameters $\pi = (\pi_1, \pi_2)$ are updated via

$$\begin{aligned} \pi(t+1) = \pi(t) - \eta_\pi \nabla_\pi \frac{1}{2} & \left\| \pi_1(t) \log(L_{\text{distill}}(\theta_t)) \right. \\ & \left. + \pi_2(t) \log(L_{\text{task}}(\theta_t)) \right\|^2. \quad (15) \end{aligned}$$

Please note that since the update in Equation (15) does not guarantee $\pi \in \Delta$, one should renormalize it via a softmax function. We have empirically observed that the amortized algorithm comfortably outperforms state-of-the-art KD algorithms with significant improvement over training speed. For example, Figure 6 shows that our approach demonstrate the faster convergence when compared to other approaches. Specifically, the MoKD reaches the top performance of [29] with 300 epochs in just 230 epochs.

3.2. Student and Teacher subspace learning

A recent study by [29] proposes to perform KD via utilizing an extra projection layer. Let $\mathbf{z}_t \in \mathbb{R}^{n_t}$ and $\mathbf{z}_s \in \mathbb{R}^{n_s}$ be the feature vectors from the teacher and student, respectively. To be able to transfer knowledge from the teacher to the student even when $n_t \neq n_s$, [29] propose learning $\mathbf{P} \in St(n_t, n_s)$ along with learning the parameters of student θ . With \mathbf{P} at disposal, the KD loss can be written as maximizing the similarity of $s(\mathbf{z}_t, \mathbf{z}_s) = \mathbf{z}_t^\top \mathbf{P} \mathbf{z}_s$. This in essence means that we learn an orthogonal projection from the teacher’s latent space to a lower dimensional latent space of the student to facilitate the transfer of knowledge. Despite the success, we propose an improvement to this notion and propose to formulate measuring the similarity between the student and teachers features as

$$s(\mathbf{z}_t, \mathbf{z}_s) = \mathbf{z}_t^\top \mathbf{P}_t^\top \mathbf{D} \mathbf{P}_s^\top \mathbf{z}_s, \quad (16)$$

where $\mathbf{P}_t \in St(n, n_t)$, $\mathbf{P}_s \in St(n, n_s)$ and $\mathbf{D} \in \mathbb{R}^{n \times n}$ is a diagonal matrix. Our idea is to enable learning in a common n dimensional latent space via two projections \mathbf{P}_t and \mathbf{P}_s . We enforce the projections to be orthogonal inline with observations in [29], which shows a structured and orthogonal projection is beneficial for KD. Please note that the

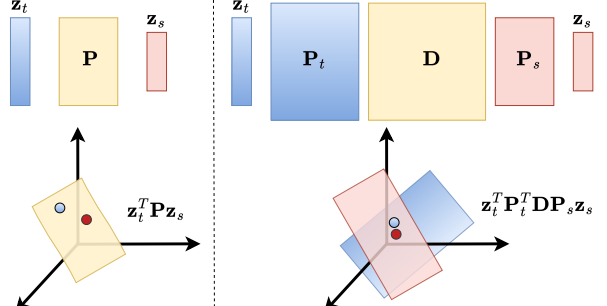


Figure 4. **Subspace learning:** Left) Learning of a single projector layer as in [29]. Right) Learning separate student and teacher subspaces, which are aligned in a high-dimensional space.

formulation via $\mathbf{P}_t^\top \mathbf{D} \mathbf{P}_s^\top$ while in the end is a mapping between \mathbb{R}^{n_t} and \mathbb{R}^{n_s} is different from having one projection as in [29]. Please refer to the appendix for further details.

4. Experiments

We evaluate our proposed method, MoKD, on two distinct vision tasks: image classification and object detection. For image classification, we adopt a CNN-based teacher model, RegNetY-160 [26], and use transformer-based DeiT [36] Small and Tiny as student models. For object detection, we employ transformer-based ViDT-Base [32] as the teacher model, with ViDT-Small, ViDT-Tiny, and ViDT-Nano serving as the student models. Additionally, to assess the robustness of our method, we conduct distillation experiments using ViDT-Small as the teacher.

Implementation details: In our approach, MoKD, we reformulate model training as a gradient-based multi-task optimization problem. For the multi-task optimization across both classification and detection tasks, we use AdamW with a learning rate of 0.025 and a weight decay of 0.01. For classification, we adopt the training strategy and parameters from DeiT [34]. Additionally, for data augmentation, we follow the method outlined in [29]. For learning, we employ AdamW [20] with a learning rate of 0.001 and a weight decay of 0.05. For object detection, we adhere to the training methodology from ViDT [32]. MoKD is trained using AdamW [20] with an initial learning rate of 10-4 for the body, neck, and head. We use the same hyperparameters as those in the ViDT [32] transformer encoder and decoder. All experiments are conducted using PyTorch [24] and executed on four NVIDIA H100 GPUs.

4.1. Object classification

We conducted extensive experiments on the ImageNet-1K dataset, using the RegNetY-160 [26] model, pre-trained on the larger ImageNet-21K dataset, as the teacher to facilitate robust knowledge transfer. Two student models, DeiT-tiny and DeiT-small, were trained for 300 epochs on ImageNet-

	ViDT Model	Epochs	AP	AP₅₀	AP₇₅	AP_S	AP_M	AP_L	#Params	FPS
Teacher	Swin-base [32]	50	49.4	69.6	53.4	31.6	52.4	66.8	0.1B	9.0
Student	Swin-nano [32]	50	40.4	59.6	43.3	23.2	42.5	55.8		
	Token-Matching [33]	50	41.9	61.2	44.7	23.6	44.1	58.7	16M	20.0
	V_kD -nano [29]	50	43.0	62.3	46.2	24.8	45.3	60.1		
	MoKD-nano	50	43.7	63.1	46.8	25.1	46.2	61.9		
Student	Swin-tiny [32]	50	44.8	64.5	48.7	25.9	47.6	62.1		
	Token-Matching [33]	50	46.6	66.3	50.4	28.0	49.5	64.3	38M	17.2
	V_kD -tiny [29]	50	46.9	66.6	50.9	27.8	49.8	64.6		
	MoKD-tiny	50	47.4	67.2	51.3	28.0	50.7	65.8		
Student	Swin-small [32]	50	47.5	67.7	51.4	29.2	50.7	64.8		
	Token-Matching [33]	50	49.2	69.2	53.6	30.7	52.3	66.8	61M	12.1
	V_kD -small [29]	50	48.5	68.4	52.4	30.8	52.2	66.0		
	MoKD-small	50	49.6	69.4	53.9	31.6	53.1	67.1		

Table 1. **Object Detection task:** Comparison with other detectors on COCO, with student models distilled from a pre-trained ViDT-base.

1K, and their performance was compared against existing state-of-the-art methods. As shown in Tab. 2, our approach demonstrates significant improvements in accuracy for both student models. Specifically, MoKD outperforms the baseline [34] by 5.2 percentage points (pp) for the tiny model and 1.9 pp for the small model. Additionally, DeiT-tiny surpasses the previous state-of-the-art method [29] by 1.4 pp, indicating a substantial enhancement in classification accuracy. For DeiT-small, our approach achieves a 0.8 pp accuracy improvement over [29].

Additionally, compared to the baseline [34], which was trained for 1000 epochs, MoKD achieves a 3.1 percentage point (pp) improvement for the tiny model and a 0.5 pp improvement for the small model with just 300 epochs. This highlights the efficiency of our approach, demonstrating its ability to deliver competitive performance in significantly less training time, making it both effective and scalable.

Due to space limitations, additional experiments with various student-teacher models and both homogeneous and heterogeneous architectures on the CIFAR-100 dataset are provided in the supplementary material.

4.2. Object detection

Tab. 1 demonstrates that our proposed method, MoKD, achieves state-of-the-art object detection performance on the MS-COCO benchmark [16], leveraging the ViDT transformer architecture [33] for its strong performance and efficiency on consumer hardware. MoKD consistently improves upon various ViDT variants, enhancing the Swin-nano backbone by 0.7 percentage points (pp), Swin-tiny by 0.5pp, and Swin-small by 1.1pp. Notably, MoKD-small, with just 61M parameters, outperforms Swin-base (0.1B parameters) when both are trained from scratch. Additionally, MoKD-tiny, with 38M parameters, achieves nearly the same performance as Swin-small (61M parameters).

4.3. Ablation studies

Impact of different components in MoKD: We conduct a thorough evaluation of the impact of each primary com-

Method	Venue	Top@1	Teacher	#Param.
RegNetY-160 [26]	CVPR20	82.6	None	84M
CaiT-S24 [35]	ICCV21	83.4	None	47M
DeiT3-B [36]	ECCV22	83.8	None	87M
DeiT-Ti [34]	ICML21	72.2	None	5M
DeiT-Ti (KD) [34]	ICML21	74.5	RegnetY-160	6M
↳ 1000 epochs	ICML21	76.6	RegnetY-160	6M
CivT-Ti [27]	CVPR22	74.9	RegnetY-600m + Rednet-26	6M
Manifold [9]	NeurIPS22	76.5	CaiT-S24	6M
DearKD [4]	CVPR22	74.8	RegnetY-160	6M
↳ 1000 epochs	CVPR22	77.0	RegnetY-160	6M
USKD [41]	ICCV23	75.0	RegnetY-160	6M
MaskedKD [31]	ECCV24	75.4	CaiT-S24	6M
SRD [21]	AAAI24	77.2	RegnetY-160	6M
V_kD -Ti [29]	CVPR24	78.3	RegnetY-160	6M
MoKD-Ti		79.7	RegnetY-160	6M
DeiT-S [34]	ICML21	79.8	None	22M
DeiT-S (KD) [34]	ICML21	81.2	RegnetY-160	22M
↳ 1000 epochs	ICML21	82.6	RegnetY-160	22M
CivT-S [27]	CVPR22	82.0	RegnetY-4gf + Rednet-50	22M
DearKD [4]	CVPR22	81.5	RegnetY-160	22M
↳ 1000 epochs	CVPR22	82.8	RegnetY-160	22M
USKD [41]	ICCV23	80.8	RegnetY-160	22M
MaskedKD [31]	ECCV24	81.4	DeiT3-B	22M
SRD [21]	AAAI24	82.1	RegnetY-160	22M
V_kD -S [29]	CVPR24	82.3	RegnetY-160	22M
MoKD-S		83.1	RegnetY-160	22M

Table 2. **Object Classification task:** Multi-objective knowledge distillation on the ImageNet-1K dataset. Unless specified, each model is only trained for 300 epochs.

Subspace Learning	Multi-Task Optimization	High-dimensional Alignment	S:MoKD-nano / T:ViDT-base
			AP
			AP ₅₀
			41.8
✓			61.2
✓	✓		44.7
✓	✓	✓	43.1
			61.7
			46.4
			43.4
			62.4
			46.5
		✓	43.7
			63.1
			46.8

Table 3. **Component’s Impact Assessment:** We evaluate the AP using ViDT-base as the teacher and MoKD-nano as the student.

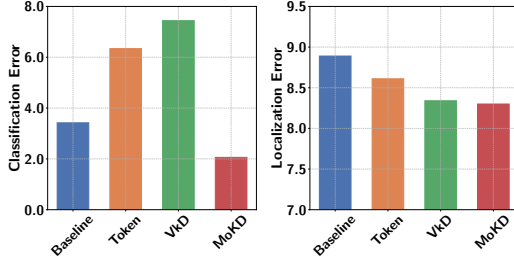


Figure 5. **Error analysis** on the object detection using ViDT-nano.

ponent in MoKD, specifically assessing subspace learning, multi-task optimization, and alignment between teacher and student subspaces. These components were introduced to enhance the knowledge distillation process, and their individual contributions are analyzed in Tab. 3. The results demonstrate that each component significantly contributes to the performance of MoKD, with all showing a positive effect on the overall effectiveness of the model. Subspace learning improves feature representation, multi-task optimization enables the model to handle diverse objectives, and alignment between teacher and student subspaces facilitates smoother knowledge transfer.

Subtask error analysis: We conduct a thorough analysis of both classification and localization errors [1] in the object detection task. MoKD outperforms other methods, achieving fewer errors in both areas while maintaining a strong balance between them. Notably, other KD techniques [29, 33] underperform in the classification subtask compared to the baseline [32], highlighting the superior effectiveness of our approach. See Fig. 5 for more details.

Distillation from different teachers: Tab. 4 demonstrates MoKD’s strong performance, even with smaller teachers like ViDT-small. This highlights its robustness, adaptability, and efficiency in resource-constrained settings, making it a versatile and effective distillation method across different teacher model scales.

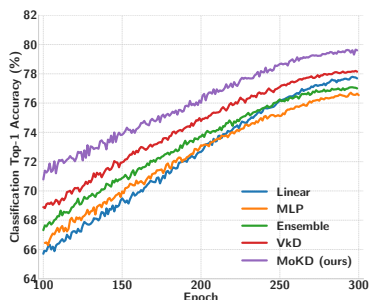


Figure 6. **Convergence analysis** of different student models trained for 300 epochs on the ImageNet-1K dataset, guided by a pre-trained RegNetY-160 as the teacher model.

Student	ViDT-nano		ViDT-tiny	
	ViDT	ViDT (small)	ViDT	ViDT (base)
No Distillation [32]	<i>ICLR21</i>		40.4	44.8
Token Matching [33]	<i>ICLR22</i>	41.5	41.9	45.8
V_kD [29]	<i>CVPR24</i>	42.2	43.0	45.9
MoKD		43.2	43.7	46.9
				47.4

Table 4. **Object Detection task:** Comparison of ViDT on COCO2017 val set. We report AP for the student models distilled from different teacher models.

Faster convergence in MoKD: We plot the top-1 accuracy over the last 200 epochs, as shown in Fig. 6. As observed, MoKD converges significantly faster than other projector-based methods. Specifically, we compare our method with linear, orthogonal, MLP [23], and Ensemble [5], following the approach in [29]. Notably, MoKD maintains its performance even with longer training schedules, showing no degradation.

5. Limitations

Like other KD methods, data availability is a bottleneck. MoKD is designed for distillation with available data, and extending it to data-free settings, especially for distilling from large pre-trained models, remains an open challenge. Extending MoKD to a data-free regime through sample synthesis may be more difficult due to its min-max optimization formulation.

6. Conclusion

MoKD offers a novel approach to tackling key challenges in distilling knowledge from large teacher models to compact student models, especially in the context of transformer architectures. By addressing the substantial disparities in feature representations between student and teacher models, MoKD introduces a powerful subspace learning technique that aligns both models within an indefinite inner product space. This alignment captures richer, more nuanced representations, including both traditional “positive” knowledge and complex, often overlooked “dark” knowledge, which is particularly valuable for transformer-based models with their deep and intricate feature spaces. Furthermore, MoKD resolves the common issue of conflicting supervision signals by reformulating distillation as a multi-task optimization problem. This formulation allows for a balanced and harmonious integration of task-specific losses (e.g., classification or detection) with the distillation loss, enabling more effective and efficient training of student models. MoKD outperforms existing distillation methods demonstrating state-of-the-art performance on image classification and object detection tasks.

References

- [1] Daniel Bolya, Sean Foley, James Hays, and Judy Hoffman. Tide: A general toolbox for identifying object detection errors. In *ECCV*, 2020. 8
- [2] Linqun Chen, Dong Wang, Zhe Gan, Jingjing Liu, Ricardo Henao, and Lawrence Carin. Wasserstein Contrastive Representation Distillation. In *CVPR*, 2020. 1
- [3] Pengguang Chen, Shu Liu, Hengshuang Zhao, and Jiaya Jia. Distilling Knowledge via Knowledge Review. In *CVPR*, 2021. 1, 2
- [4] Xianing Chen, Qiong Cao, Yujie Zhong, Jing Zhang, Shenghua Gao, and Dacheng Tao. Dearkd: Data-efficient early knowledge distillation for vision transformers. In *CVPR*, 2022. 1, 2, 3, 7
- [5] Yudong Chen, Sen Wang, Jiajun Liu, Xuwei Xu, Frank de Hoog, and Zi Huang. Improved Feature Distillation via Projector Ensemble. In *NeurIPS*, 2022. 8
- [6] Zhao Chen, Vijay Badrinarayanan, Chen-Yu Lee, and Andrew Rabinovich. GradNorm: Gradient normalization for adaptive loss balancing in deep multitask networks. In *ICML*, 2018. 3
- [7] Pengguang Chen et al. Distilling knowledge via knowledge review. In *CVPR*, 2021. 14
- [8] Mengya Gao, Yujun Shen, Quanquan Li, Junjie Yan, Liang Wan, Dahua Lin, Chen Change Loy, and Xiaoou Tang. An Embarrassingly Simple Approach for Knowledge Distillation. *arXiv*, 2018. 1
- [9] Zhiwei Hao, Jianyuan Guo, Ding Jia, Kai Han, Yehui Tang, Chao Zhang, Han Hu, and Yunhe Wang. Learning efficient vision transformers via fine-grained manifold distillation. In *NeurIPS*, 2022. 3, 7
- [10] Byeongho Heo, Jeesoo Kim, Sangdoo Yun, Hyojin Park, Nojun Kwak, and Jin Young Choi. A comprehensive overhaul of feature distillation. In *ICCV*, 2019. 1, 2
- [11] Geoffrey Hinton, Oriol Vinyals, and Jeff Dean. Distilling the Knowledge in a Neural Network. In *NeurIPS*, 2015. 1, 2
- [12] Chengming Hu, Haolun Wu, Xuan Li, Chen Ma, Xi Chen, Jun Yan, Boyu Wang, and Xue Liu. Less or more from teacher: Exploiting trilateral geometry for knowledge distillation. In *ICLR*, 2024. 3
- [13] Tao Huang, Yuan Zhang, Mingkai Zheng, Shan You, Fei Wang, Chen Qian, and Chang Xu. Knowledge diffusion for distillation. In *NeurIPS*, 2024. 3
- [14] Alex Kendall, Yarin Gal, and Roberto Cipolla. Multi-task learning using uncertainty to weigh losses for scene geometry and semantics. In *CVPR*, 2018. 3
- [15] Jiguan Lin. Multiple-objective problems: Pareto-optimal solutions by method of proper equality constraints. *IEEE Transactions on Automatic Control*, 1976. 2
- [16] Tsung Yi Lin, Michael Maire, Serge Belongie, James Hays, Pietro Perona, Deva Ramanan, Piotr Dollár, and C. Lawrence Zitnick. Microsoft COCO: Common objects in context. In *ECCV*, 2014. 7
- [17] Bo Liu, Xingchao Liu, Xiaojie Jin, Peter Stone, and Qiang Liu. Conflict-averse gradient descent for multi-task learning. In *NeurIPS*, 2021. 3, 11
- [18] Bo Liu, Yihao Feng, Peter Stone, and Qiang Liu. Famo: Fast adaptive multitask optimization. In *NeurIPS*. Curran Associates, Inc., 2023. 3, 5, 6
- [19] Liyang Liu, Yi Li, Zhanghui Kuang, J Xue, Yimin Chen, Wenming Yang, Qingmin Liao, and Wayne Zhang. Towards impartial multi-task learning. In *ICLR*, 2021. 3, 11
- [20] Ilya Loshchilov and Frank Hutter. Decoupled weight decay regularization. In *ICLR*, 2019. 6
- [21] Roy Miles and Krystian Mikolajczyk. Understanding the role of the projector in knowledge distillation. In *AAAI*, 2024. 2, 3, 7
- [22] Seyed-Iman Mirzadeh, Mehrdad Farajtabar, Ang Li, and Hassan Ghasemzadeh. Improved Knowledge Distillation via Teacher Assistant: Bridging the Gap Between Student and Teacher. In *AAAI*, 2020. 2
- [23] K L Navaneet, Soroush Abbasi Koohpayegani, Ajinkya Tejankar, and Hamed Pirsiavash. SimReg: Regression as a Simple Yet Effective Tool for Self-supervised Knowledge Distillation. In *BMVC*, 2021. 8
- [24] Adam Paszke, Sam Gross, Soumith Chintala, Gregory Chanan, Edward Yang, Zachary DeVito, Zeming Lin, Alban Desmaison, Luca Antiga, and Adam Lerer. Automatic differentiation in pytorch. In *NeurIPS*, 2017. 6
- [25] Zengyu Qiu, Xinzhu Ma, Kunlin Yang, Chunyu Liu, Jun Hou, Shuai Yi, and Wanli Ouyang. Better teacher better student: Dynamic prior knowledge for knowledge distillation. In *ICLR*, 2023. 1
- [26] Ilija Radosavovic, Raj Prateek Kosaraju, Ross Girshick, Kaiming He, and Piotr Dollár. Designing Network Design Spaces. In *CVPR*, 2020. 6, 7
- [27] Sucheng Ren, Zhengqi Gao, Tianyu Hua, Zihui Xue, Yonglong Tian, Shengfeng He, and Hang Zhao. Co-advise: Cross Inductive Bias Distillation. In *CVPR*, 2022. 3, 7
- [28] Adriana Romero, Nicolas Ballas, Samira Ebrahimi Kahou, Antoine Chassang, Carlo Gatta, and Yoshua Bengio. FitNets: Hints For Thin Deep Nets. In *ICLR*, 2015. 1, 2
- [29] Ismail Elezi Roy Miles and Jiankang Deng. Vkd : Improving knowledge distillation using orthogonal projections. In *CVPR*, 2024. 1, 2, 3, 4, 6, 7, 8, 13, 14
- [30] Ozan Sener and Vladlen Koltun. Multi-task learning as multi-objective optimization. In *NeurIPS*, 2018. 3, 11
- [31] Seungwoo Son, Namhoon Lee, and Jaeho Lee. Maskedkd: Efficient distillation of vision transformers with masked images. In *ECCV*, 2024. 2, 7
- [32] Hwanjun Song, Deqing Sun, Sanghyuk Chun, Varun Jampani, Dongyoon Han, Byeongho Heo, Wonjae Kim, and Ming-Hsuan Yang. Vidt: An efficient and effective fully transformer-based object detector. In *ICLR*, 2021. 3, 6, 7, 8, 13
- [33] Hwanjun Song, Deqing Sun, Sanghyuk Chun, Varun Jampani, Dongyoon Han, Byeongho Heo, Wonjae Kim, and Ming-Hsuan Yang. Vidt: An efficient and effective fully transformer-based object detector. In *ICLR*, 2022. 2, 3, 7, 8
- [34] Hugo Touvron, Matthieu Cord, Matthijs Douze, Francisco Massa, Alexandre Sablayrolles, and Hervé Jégou. Training data-efficient image transformers & distillation through attention. In *PMLR*, 2021. 6, 7

- [35] Hugo Touvron, Matthieu Cord, Alexandre Sablayrolles, Gabriel Synnaeve, and Hervé Jégou. Going deeper with image transformers. In *ICCV*, 2021. 7
- [36] Hugo Touvron, Matthieu Cord, and Hervé Jégou. Deit iii: Revenge of the vit. In *ECCV*, 2022. 3, 6, 7
- [37] Jiaobao Wang, Yuming Chen, Zhaohui Zheng, Xiang Li, Ming-Ming Cheng, and Qibin Hou. Crosskd: Cross-head knowledge distillation for object detection. In *CVPR*, 2024. 2
- [38] Yuzhu Wang et al. Improving knowledge distillation via regularizing feature direction and norm. In *ECCV*, 2024. 3, 14
- [39] Guodong Xu, Ziwei Liu, Xiaoxiao Li, and Chen Change Loy. Knowledge distillation meets self-supervision. *ECCV*, 2020. 2
- [40] Chuanguang Yang, Zhulin An, Linhang Cai, and Yongjun Xu. Hierarchical self-supervised augmented knowledge distillation. In *Proceedings of the Thirtieth International Joint Conference on Artificial Intelligence (IJCAI)*, pages 1217–1223, 2021. 2
- [41] Zhendong Yang, Ailing Zeng, Zhe Li, Tianke Zhang, Chun Yuan, and Yu Li. From knowledge distillation to self-knowledge distillation: A unified approach with normalized loss and customized soft labels. In *ICCV*, 2023. 3, 7
- [42] Junho Yim. A Gift from Knowledge Distillation: Fast Optimization, Network Minimization and Transfer Learning. In *CVPR*, 2017. 1
- [43] Nicholas Young. *An introduction to Hilbert space*. Cambridge university press, 1988. 3
- [44] Tianhe Yu, Saurabh Kumar, Abhishek Gupta, Sergey Levine, Karol Hausman, and Chelsea Finn. Gradient surgery for multi-task learning. In *NeurIPS*, 2020. 3, 11
- [45] Ying Zhang, Tao Xiang, Timothy M. Hospedales, and Huchuan Lu. Deep Mutual Learning. In *CVPR*, 2018. 1, 2
- [46] Borui Zhao, Quan Cui, Renjie Song, Yiyu Qiu, and Jiajun Liang. Decoupled knowledge distillation. In *CVPR*, 2022. 2
- [47] Kaixiang Zheng and En-Hui Yang. Knowledge distillation based on transformed teacher matching. In *The Twelfth International Conference on Learning Representations (ICLR 2024)*, 2024. 3
- [48] Zaida Zhou, Chaoran Zhuge, Xinwei Guan, and Wen Liu. Channel Distillation: Channel-Wise Attention for Knowledge Distillation. In *ICCV*, 2020. 1

A. Multi-task knowledge distillation

In this paper, we approach knowledge distillation as a multi-task optimization problem. We design a framework that allows us to learn the weights for each task dynamically. To achieve this, we leverage gradient manipulation methods [17–19, 30, 44], which enable us to adjust these weights effectively throughout training. As a result, we formulate the knowledge distillation for classification as a multi-objective optimization problem as:

$$\mathbf{L}_t^{cls} \triangleq \begin{pmatrix} \mathbf{L}_{\text{distill}} \\ \mathbf{L}_{\text{task}} \end{pmatrix} = \begin{pmatrix} \mathbf{L}_{\text{kl}} + \mathbf{L}_{\text{kd}} \\ \mathbf{L}_{\text{cls}} \end{pmatrix}. \quad (1)$$

We note that $\mathbf{L}_t^{cls} \in \mathbb{R}_+^2$ is a vector representing the objective of learning. Furthermore, \mathbf{L}_{kd} and \mathbf{L}_{kl} are the KL-divergence loss and normalized L1 loss respectively. We follow a similar approach for distilling knowledge for the object detection task with the following loss:

$$\mathbf{L}_t^{det} = \begin{pmatrix} \mathbf{L}_{\text{distill}} \\ \mathbf{L}_{\text{task}} \end{pmatrix} = \begin{pmatrix} \mathbf{L}_{\text{patch}} + \mathbf{L}_{\text{neck}} + \mathbf{L}_{\text{head}} \\ \mathbf{L}_{\text{cls}} + \mathbf{L}_{\text{bbox}} + \mathbf{L}_{\text{giou}} \end{pmatrix} \quad (2)$$

Remark A.1. One could formulate the object detection problem as optimizing an objective with several tasks such as $\mathbf{L}_t^{det} \triangleq \left(\mathbf{L}_{\text{patch}} + \mathbf{L}_{\text{neck}} + \mathbf{L}_{\text{head}}, \mathbf{L}_{\text{cls}}, \mathbf{L}_{\text{bbox}} + \mathbf{L}_{\text{giou}} \right)^\top$ or the object classification task as $\mathbf{L}_t^{cls} \triangleq \left(\mathbf{L}_{\text{kl}}, \mathbf{L}_{\text{kd}}, \mathbf{L}_{\text{cls}} \right)^\top$. Empirically, we observe that the losses that belong to the same task generally perform better when learned together, as shown in Eq. (1) and Eq. (2).

This multi-task knowledge distillation approach is detailed in Algorithm 1. The task weights $\boldsymbol{\pi}$ are initialized to 0. The *DistillHead* and *TaskHead* refer to specific heads learning distillation and the task, respectively. Also, the color scheme in Algorithm 1 reflects the color scheme of different components of our pipeline, as shown in Figure (2) of the main paper.

B. Theoretical analysis

In this section, we provide a detailed formulation for the closed-form solution.

Theorem B.1 (Closed Form Solution). *Let $\mathbf{J}_t = [\nabla \log(L_{\text{distill}}(\boldsymbol{\theta}_t)), \nabla \log(L_{\text{task}}(\boldsymbol{\theta}_t))] \in \mathbb{R}^{n \times 2}$. The closed-form solution to the optimization problem*

$$\begin{aligned} \boldsymbol{\pi}^* &\in \arg \min_{\boldsymbol{\pi}} \frac{1}{2} \|\mathbf{J}_t \boldsymbol{\pi}\|^2 \\ \text{s.t. } &\pi_1 + \pi_2 = 1 \end{aligned} \quad (3)$$

Algorithm 1 Multi-task Knowledge Distillation

```

1: Inputs: Dataset  $\mathcal{S} = \{(\mathbf{x}_i, \mathbf{y}_i), \dots\}$ ; Teacher  $f_t$ 
2: Initialise: Student  $f_s$  with  $\theta$ ; Task weight  $\boldsymbol{\pi} \leftarrow \frac{1}{2}$ 
3: for  $t = 1 : T$  do (iterations)
4:    $\mathbf{x}_\tau, \mathbf{y}_\tau = \{(\mathbf{x}_b, \mathbf{y}_b)\}_{b=1}^B \sim \mathcal{S}$  (batch)
5:    $\mathbf{z}_t, \mathbf{z}_s \leftarrow f_t(\mathbf{x}_\tau), f_s(\mathbf{x}_\tau)$  (latent features)
6:    $\hat{\mathbf{z}}_t, \hat{\mathbf{z}}_s \leftarrow \mathbf{z}_t^\top \mathbf{P}_t^T \mathbf{D} \mathbf{P}_s^\top \mathbf{z}_s$  (subspace)
7:    $\mathbf{L}_t = \begin{bmatrix} \mathbf{L}_{\text{distill}} \\ \mathbf{L}_{\text{task}} \end{bmatrix} = \begin{bmatrix} \ell_{\text{distill}}(\text{DistillHead}(\hat{\mathbf{z}}_s, \hat{\mathbf{z}}_t)) \\ \ell_{\text{task}}(\text{TaskHead}(\mathbf{z}_s, \mathbf{y}_\tau)) \end{bmatrix}$  (loss vector)
8:    $\mathbf{g}_t = \pi_1 \nabla \log(\mathbf{L}_{\text{distill}}(\boldsymbol{\theta}_t)) + \pi_2 \nabla \log(\mathbf{L}_{\text{task}}(\boldsymbol{\theta}_t))$ 
9:    $\boldsymbol{\theta}_{t+1} = \boldsymbol{\theta}_t - \gamma \mathbf{g}_t$  (student model learning)
10:   $\mathbf{L}_{t+1} \leftarrow f_s(\mathbf{x}_\tau)$  (frozen model inference)
11:   $\mathbf{r}(\mathbf{g}_t) = \begin{bmatrix} r_{\text{distill}}(\mathbf{g}_t) \\ r_{\text{task}}(\mathbf{g}_t) \end{bmatrix} = \begin{bmatrix} \frac{\mathbf{L}_{\text{distill}}(\boldsymbol{\theta}_t) - \mathbf{L}_{\text{distill}}(\boldsymbol{\theta}_{t+1})}{\mathbf{L}_{\text{distill}}(\boldsymbol{\theta}_t) - \mathbf{L}_{\text{distill}}(\boldsymbol{\theta}_{t+1})} \\ \frac{\mathbf{L}_{\text{task}}(\boldsymbol{\theta}_t) - \mathbf{L}_{\text{task}}(\boldsymbol{\theta}_{t+1})}{\mathbf{L}_{\text{task}}(\boldsymbol{\theta}_t)} \end{bmatrix}$  (update direction)
12:   $\mathbf{J}_t = [\nabla \log(\mathbf{L}_{\text{distill}}(\boldsymbol{\theta}_t)) \mid \nabla \log(\mathbf{L}_{\text{task}}(\boldsymbol{\theta}_t))]^\top$  (task gradient)
13:   $\boldsymbol{\pi}_t^* \in \arg \min_{\boldsymbol{\pi} \in \Delta} \frac{1}{2} \|\mathbf{J}_t \boldsymbol{\pi}\|^2$  (optimize weights)

```

is given by

$$\pi_1^* = \frac{g_{22} - g_{12}}{g_{11} + g_{22} - 2g_{12}}, \quad (4)$$

$$\pi_2^* = \frac{g_{11} - g_{12}}{g_{11} + g_{22} - 2g_{12}}, \quad (5)$$

where $\mathbf{G} = \mathbf{J}_t^\top \mathbf{J}_t$ is the Gram matrix:

$$\mathbf{G} = \begin{bmatrix} g_{11} & g_{12} \\ g_{21} & g_{22} \end{bmatrix},$$

with elements

$$g_{11} = \|\nabla \log(\mathbf{L}_{\text{distill}}(\boldsymbol{\theta}_t))\|^2,$$

$$g_{12} = g_{21} = \langle \nabla \log(\mathbf{L}_{\text{distill}}(\boldsymbol{\theta}_t)), \nabla \log(\mathbf{L}_{\text{task}}(\boldsymbol{\theta}_t)) \rangle,$$

$$g_{22} = \|\nabla \log(\mathbf{L}_{\text{task}}(\boldsymbol{\theta}_t))\|^2.$$

Proof. Using the constraint $\pi_2 = 1 - \pi_1$, we can expand the objective function as follows:

$$\begin{aligned} \frac{1}{2} \|\mathbf{J}_t \boldsymbol{\pi}\|^2 &= \frac{1}{2} \|\pi_1 \nabla \log(\mathbf{L}_{\text{distill}}(\boldsymbol{\theta}_t)) + \pi_2 \nabla \log(\mathbf{L}_{\text{task}}(\boldsymbol{\theta}_t))\|^2 \\ &= \frac{1}{2} (\pi_1^2 g_{11} + \pi_2^2 g_{22} + 2\pi_1 \pi_2 g_{12}) \\ &= \frac{1}{2} (\pi_1^2 g_{11} + (1 - \pi_1)^2 g_{22} + 2\pi_1 (1 - \pi_1) g_{12}) \end{aligned}$$

Taking the derivative with respect to π_1 and setting it to zero:

$$\begin{aligned} \frac{d}{d\pi_1} \frac{1}{2} (\pi_1^2 g_{11} + (1 - \pi_1)^2 g_{22} + 2\pi_1(1 - \pi_1)g_{12}) &= \\ \pi_1(g_{11} + g_{22} - 2g_{12}) - g_{22} + g_{12} \\ \implies \boxed{\pi_1^* = \frac{g_{22} - g_{12}}{g_{11} + g_{22} - 2g_{12}}}. \end{aligned}$$

Using the fact that $\pi_1 + \pi_2 = 1$, we obtain

$$\pi_2^* = \frac{g_{11} - g_{12}}{g_{11} + g_{22} - 2g_{12}}.$$

□

Corollary B.2 (Alignment of \mathbf{g}^*). *Define $\mathbf{g}_1 = \nabla \log(L_{\text{distill}}(\theta_t))$ and $\mathbf{g}_2 = \nabla \log(L_{\text{task}}(\theta_t))$. Then the update direction $\mathbf{g}^* = \pi_1 \mathbf{g}_1 + \pi_2 \mathbf{g}_2$ for π^* defined in Equation (4) is aligned with both \mathbf{g}_1 and \mathbf{g}_2 .*

Proof. Assume that \mathbf{g}_1 and \mathbf{g}_2 are in conflict (i.e., $-1 < \langle \mathbf{g}_1, \mathbf{g}_2 \rangle < 0$). We study the behavior of $\langle \mathbf{g}^*, \mathbf{g}_1 \rangle$ and $\langle \mathbf{g}^*, \mathbf{g}_2 \rangle$ below.

$$\begin{aligned} \langle \mathbf{g}^*, \mathbf{g}_1 \rangle &= \langle \pi_1 \mathbf{g}_1 + \pi_2 \mathbf{g}_2, \mathbf{g}_1 \rangle = \pi_1 \|\mathbf{g}_1\|^2 + \pi_2 \langle \mathbf{g}_2, \mathbf{g}_1 \rangle \\ &= \frac{g_{22} - g_{12}}{g_{11} + g_{22} - 2g_{12}} g_{11} + \frac{g_{11} - g_{12}}{g_{11} + g_{22} - 2g_{12}} g_{12} \\ &= \frac{g_{11}g_{22} - g_{12}^2}{\|\mathbf{g}_1 - \mathbf{g}_2\|^2} \end{aligned}$$

Similarly, for \mathbf{g}_2 :

$$\begin{aligned} \langle \mathbf{g}^*, \mathbf{g}_2 \rangle &= \langle \pi_1 \mathbf{g}_1 + \pi_2 \mathbf{g}_2, \mathbf{g}_2 \rangle = \pi_1 \langle \mathbf{g}_1, \mathbf{g}_2 \rangle + \pi_2 \|\mathbf{g}_2\|^2 \\ &= \frac{g_{22} - g_{12}}{g_{11} + g_{22} - 2g_{12}} g_{12} + \frac{g_{11} - g_{12}}{g_{11} + g_{22} - 2g_{12}} g_{22} \\ &= \frac{g_{11}g_{22} - g_{12}^2}{\|\mathbf{g}_1 - \mathbf{g}_2\|^2}. \end{aligned}$$

Note that $g_{11}g_{22} - g_{12}^2 = \det(\mathbf{J}^\top \mathbf{J})$ and since $\mathbf{G} = \mathbf{J}^\top \mathbf{J}$ is always positive semi-definite, then $\det(\mathbf{J}^\top \mathbf{J}) \geq 0$. This proves that \mathbf{g}^* is always positively aligned with both \mathbf{g}_1 and \mathbf{g}_2 . □

Corollary B.3 (Equal Contribution of \mathbf{g}^* to Both Losses). *In Corollary B.2, we showed that*

$$\langle \mathbf{g}^*, \mathbf{g}_1 \rangle = \langle \mathbf{g}^*, \mathbf{g}_2 \rangle = \frac{g_{11}g_{22} - g_{12}^2}{\|\mathbf{g}_1 - \mathbf{g}_2\|^2}.$$

This implies that the update direction contributes equally to the descent of both the distillation and task losses, effectively mitigating gradient dominance.

Corollary B.4 (Lower Bound on $\|\mathbf{g}^*\|$). *The norm of the optimal update direction \mathbf{g}^* satisfies the lower bound:*

$$\|\mathbf{g}^*\| \geq \frac{1}{\sqrt{2}} \min(\|\mathbf{g}_1\|, \|\mathbf{g}_2\|). \quad (6)$$

This implies that the update magnitude remains controlled and does not collapse under gradient imbalance.

Proof. We have:

$$\|\mathbf{g}^*\|^2 = \frac{\|\mathbf{g}_1\|^2 \|\mathbf{g}_2\|^2}{\|\mathbf{g}_1 - \mathbf{g}_2\|^2}.$$

Note that $\|\mathbf{g}_1 - \mathbf{g}_2\|^2 \leq \|\mathbf{g}_1\|^2 + \|\mathbf{g}_2\|^2$ and hence

$$\|\mathbf{g}^*\|^2 \geq \frac{\|\mathbf{g}_1\|^2 \|\mathbf{g}_2\|^2}{\|\mathbf{g}_1\|^2 + \|\mathbf{g}_2\|^2}.$$

Without loss of generality, assume $\|\mathbf{g}_1\| \leq \|\mathbf{g}_2\|$. We have

$$\begin{aligned} \|\mathbf{g}^*\|^2 &\geq \frac{\|\mathbf{g}_1\|^2 \|\mathbf{g}_2\|^2}{\|\mathbf{g}_1\|^2 + \|\mathbf{g}_2\|^2} \\ &\geq \frac{\|\mathbf{g}_1\|^2 \|\mathbf{g}_2\|^2}{2 \max(\|\mathbf{g}_1\|^2, \|\mathbf{g}_2\|^2)} = \frac{1}{2} \min(\|\mathbf{g}_1\|^2, \|\mathbf{g}_2\|^2) \end{aligned}$$

As such,

$$\|\mathbf{g}^*\| \geq \frac{1}{\sqrt{2}} \min(\|\mathbf{g}_1\|, \|\mathbf{g}_2\|).$$

Thus, the update direction always maintains a lower bound, ensuring that it does not collapse even when one gradient is small. □

Corollary B.5 (Upper Bound on $\|\mathbf{g}^*\|$). *The norm of the optimal update direction \mathbf{g}^* satisfies the upper bound:*

$$\|\mathbf{g}^*\| \leq \frac{\|\mathbf{g}_1\| \|\mathbf{g}_2\|}{\|\mathbf{g}_1 - \mathbf{g}_2\|}. \quad (7)$$

As such, the magnitude of the updates does not grow excessively when the gradients have different scales.

Proof. Note that

$$\begin{aligned} \|\mathbf{g}_1 - \mathbf{g}_2\|^2 &= \|\mathbf{g}_1\|^2 + \|\mathbf{g}_2\|^2 \\ -2 \underbrace{\langle \mathbf{g}_1, \mathbf{g}_2 \rangle}_{\leq \|\mathbf{g}_1\| \|\mathbf{g}_2\|} &\geq (\|\mathbf{g}_1\| - \|\mathbf{g}_2\|)^2. \end{aligned}$$

Hence

$$\begin{aligned} \|\mathbf{g}^*\|^2 &= \frac{\|\mathbf{g}_1\|^2 \|\mathbf{g}_2\|^2}{\|\mathbf{g}_1 - \mathbf{g}_2\|^2} \leq \frac{\|\mathbf{g}_1\|^2 \|\mathbf{g}_2\|^2}{(\|\mathbf{g}_1\| - \|\mathbf{g}_2\|)^2} \\ \implies \|\mathbf{g}^*\| &\leq \frac{\|\mathbf{g}_1\| \|\mathbf{g}_2\|}{\|\mathbf{g}_1 - \mathbf{g}_2\|}. \end{aligned}$$

□

C. Quantitative analysis

C.1. MoKD v.s. VkD

As seen in Fig. 1, our proposed method, MoKD, shows faster convergence using the ViDT-nano backbone [32]. Specifically, MoKD can achieve a similar performance in 20 epochs which the VkD model achieves in 28, which shows MoKD can quickly learn from the teacher model

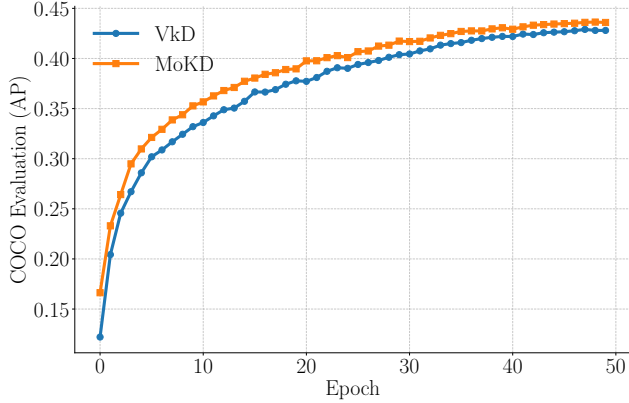


Figure 1. **Object Detection task:** MoKD-nano consistently outperforms the V_kD -nano [29] baseline distillation model.

C.2. Convergence of MoKD detection models

In Fig. 2, we plot the convergence of different MoKD student models (MoKD-nano, MoKD-tiny, and MoKD-small) as they distill knowledge from a ViDT-base model acting as the teacher. Note that in just 40 epochs, MoKD-small, with only 61M parameters, achieves the same 50-epoch performance of the ViDT-base model with 0.1B parameters.

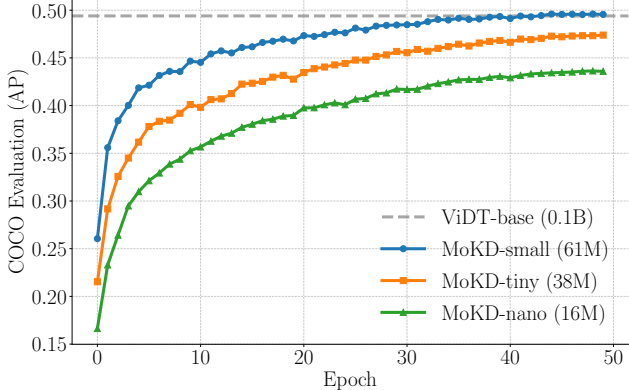


Figure 2. **Convergence of MoKD Detection models:** Distillation of different MoKD student models using ViDT-base as a teacher.

C.3. Dynamic Balancing Strategy and π values

To better illustrate our approach, the figure below shows the varying weighting ratios of the distillation loss ($\pi_{distill}$) and the task losses (π_{task}) during training. In (a), the gradient-based vector optimization in MoKD initially focuses on prioritizing the distillation loss and gradually shifts to emphasize the task losses. As illustrated in (b), we experimented with three different losses to assess the dynamic weighting for classification, with MoKD effectively learning to balance all three losses through adaptive learning.

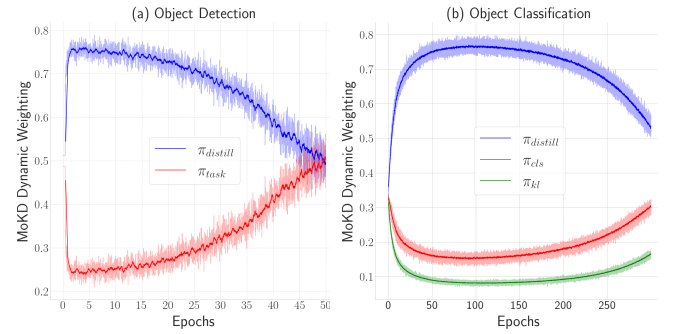


Figure 3. **Dynamic Balancing:** Left) Object detection is trained using two tasks. Right) Object classification is trained using three tasks to show that MoKD is robust to multiple tasks as well.

C.4. Gradient Analysis

We plot Gradient conflict (GrC) and gradient dominance (GrD) for our method and [29] for 500 iterations on the object detection task. The results show that our approach has less gradient conflict and exhibits less gradient dominance issue, as shown in Appendix C.4

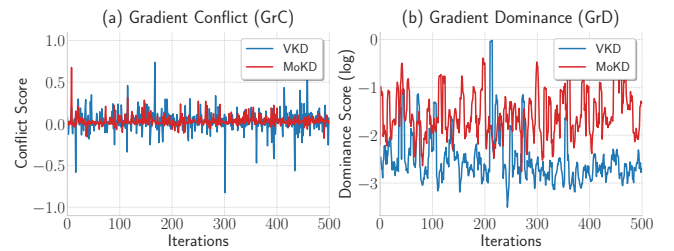


Figure 4. **Gradient Dynamics analysis.** a) Conflict score is calculated as $\langle \mathbf{g}_{distill}, \mathbf{g}_{task} \rangle$. A negative score shows strong disagreement. b) The dominance score is calculated as $\frac{\|\mathbf{g}_{distill}\|}{\|\mathbf{g}_{task}\|}$ and plotted in log-scale. The lower score represents strong dominance.

C.5. CIFAR Experiments

Experiments with various student-teacher models and homogeneous and heterogeneous architectures were con-

ducted. We benchmarked MoKD against prior KD works, following [7, 38], using the CIFAR-100. The table below shows that MoKD also achieves superior results and reinforces its superiority, establishing a new SOTA in this setting by outperforming previous works in both small- and large-dataset settings.

Methods	Homogeneous			Heterogeneous		
	ResNet-56	WRN-40-2	ResNet-32×4	ResNet-50	ResNet-32×4	ResNet-32×4
	ResNet-20	WRN-40-1	ResNet-8×4	MobileNet-V2	ShuffleNet-V1	ShuffleNet-V2
Teacher	72.34	75.61	79.42	79.34	79.42	79.42
Student	69.06	71.98	72.50	64.60	70.50	71.82
FitNet	69.21	72.24	73.50	63.16	73.59	73.54
RKD	69.61	72.22	71.90	64.43	72.28	73.21
PKT	70.34	73.45	73.64	66.52	74.10	74.69
OFD	70.98	74.33	74.95	69.04	75.98	76.82
CRD	71.16	74.14	75.51	69.11	75.11	75.65
ReviewKD [7]	71.89	75.09	75.63	69.89	77.45	77.78
ReviewKD++ [38]	72.05	75.66	76.07	70.45	77.68	77.93
MoKD (ours)	72.29	75.54	76.34	70.87	77.92	78.11

Table 1. **CIFAR-100**: Object classification benchmark using various student-teacher models and homogeneous and heterogeneous architectures.

D. Qualitative analysis

We visualize the attention maps of the final block preceding the classification head to better understand our proposed method’s behaviour. As illustrated in Fig. 5, the attention maps generated by MoKD exhibit a stronger focus on the salient object as compared to those produced by the V_kD method. Notably, MoKD demonstrates a superior ability to disregard irrelevant background elements, thereby maintaining a more concentrated and precise representation of the target object. This highlights the robustness of our approach to background noise and its effectiveness in isolating critical features.

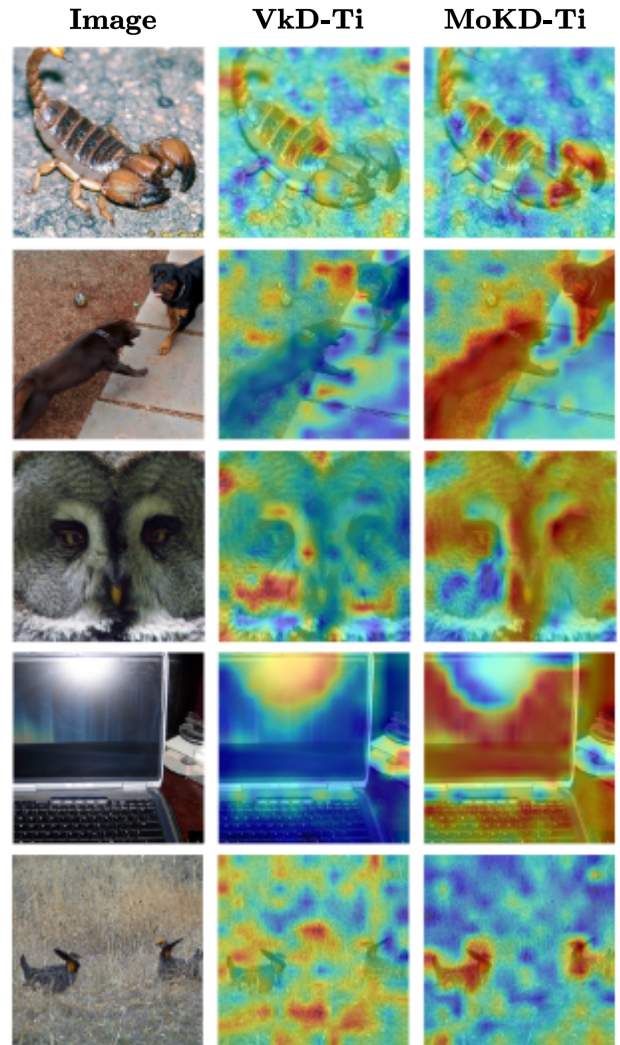


Figure 5. **Attention Map of Object Classification task**: Visualization of attention maps with tiny backbone using V_kD -tiny [29] and MoKD.